

# Estimation of the impact of geometrical uncertainties on aerodynamic coefficients using CFD

F. Chalot<sup>1</sup>, Q.V. Dinh<sup>2</sup>, E. Herbin<sup>3</sup>, L. Martin<sup>4</sup>, M. Ravachol<sup>5</sup> and G. Rogé<sup>6</sup>.  
*Dassault-Aviation, 78 quai Marcel Dassault, 92214 Saint-Cloud, France*

*Special session: Non-deterministic Simulations in Computational Fluid Dynamics*

**This paper presents two methods to propagate the uncertainties about geometrical parameters through a CFD simulation. First, the Moments method is presented and details on how to compute the necessary derivatives are provided. Secondly, surrogate models are introduced for Monte Carlo simulations. Finally, the two methods are compared for a high lift configuration and a transonic airfoil.**

## Nomenclature

$E(x)$	=	expected value of the random variable $x$
$var(x)$	=	variance of the random variable $x$
$cov(x,y)$	=	covariance of the random variables $x$ and $y$ .
$n$	=	number of random inputs
$\alpha$	=	angle of attack
$C_z$	=	lift coefficient
$C_x$	=	drag coefficient
$RBF$	=	Radial Basis Functions

## I. Introduction

One of the primary reasons for the rising interest in uncertainties management is its application in risk-based design methods. This concern is relatively new in the CFD community and can probably be explained by the relatively new use of CFD in design (especially compared to structural design) and its computational cost. In the context of CFD, the uncertainties are usually separated into two sources (Ref. 1): uncertainties due to the physical model and uncertainties due to the boundary conditions, the operating conditions or more generally the input of the computation.

For the first type, the source is usually a lack of knowledge of the actual physical behaviour. In CFD, the model with the greatest amount of uncertainty is most probably the turbulence model because turbulence is not a fully understood phenomenon leading to models which are a drastic simplification of the physics. In this case, we are technically dealing with “errors” since these uncertainties originate in either an acknowledged deliberate simplification or an acknowledged lack of understanding. However, since the exact solution is unknown, the errors can not be corrected and we have no alternative but to treat them in a non-deterministic manner as uncertainties. A valid model can also introduce uncertainties through the value of its parameters which can be either unknown or known only in a probabilistic manner.

Some inputs of the computation can be viewed as true aleatoric variables. Among the possible variations we can list the actual shape of the geometry, the atmospheric conditions (temperature, pressure, density, wind,...) and the operating conditions.

---

<sup>1</sup> Senior Scientist, Aerodynamics, member AIAA.

<sup>2</sup> Senior Scientist, Scientific Studies.

<sup>3</sup> Senior Scientist, Scientific Studies.

<sup>4</sup> Ph. D. student.

<sup>5</sup> Senior Scientist, Scientific Studies, member AIAA.

<sup>6</sup> Senior Scientist, Aerodynamics, member AIAA.

The focus of this paper is the treatment of uncertain geometrical variables. The uncertainties regarding the geometrical variables can arise from many sources: tolerance of the manufacturing process, uncertainties about the actual material properties of some elements, evolution of the geometry along the life of the aircraft (ice, damage, wear), deformations due to loads, etc. ...

Part of the work is carried out within the European project NODESIM (*Non-Deterministic Simulation for CFD-based Design Methodologies*). The objectives of the NODESIM project are to define a methodology and develop tools which will allow us to mathematically represent the uncertain parameters of interest and to propagate them throughout the mathematical model.

In our case, the uncertain parameters are *inputs* of the computation and are represented by random variables whereas we are interested in a statistical description of the *outputs* of the computation. Depending on the purpose of the final use, a central tendency may suffice, probabilities may be needed or even the probability density function of the outputs may be required. Here, we restrict ourselves within the "Robust Design" framework. A Robust Design can be viewed as a design which is relatively insensitive to *small* changes in the uncertain parameters, and information about the mean and variance of the outputs is the primary interest. Some way of extending the present methodology to Reliable Design are addressed. A Reliable Design can be defined as a design that has a probability of failure that is less than a *small* acceptable value. Dealing with the tail of probability density functions requires specific methods not discussed here, but which can benefit from the tools presented below.

To obtain the statistical description of the outputs, a straightforward manner would be to perform a Monte-Carlo simulation. Such a brute force approach, even though applicable in the simplified 2D cases considered here, does not seem to be applicable in a near future for an actual design process which involves full 3D computations. Thus, we have to consider alternate approaches, namely the moments method and Monte Carlo simulations using surrogate models.

## II. Moments method

The moments method for uncertainties propagation has been used for a long time in the risk management community. This method is very attractive for CFD applications since it only needs one deterministic nonlinear computation (CPU intensive) to estimate the mean and the standard deviation of the output. The major impediment in its practical use was that it requires the derivatives (Jacobian or Hessian matrix) of the output with respect to the fluctuating parameters. The advances in Automatic Differentiation enable one to easily calculate the needed derivatives and the moments method is becoming feasible for CFD applications (Ref. 2, 3 and 4 for example).

### A. Calculation of the moments.

The moments method is based on a Taylor expansion of the response about the mean of the input parameters. Let  $y = f(x)$  denote the random output of a *deterministic* process  $f$  with *random* inputs  $x = \{x_i\}_{i=1,\dots,n}$ . The Taylor expansion can be either a first order expansion (First order method) or a second order expansion (Second order method). A second order Taylor expansion of the output  $y$  about the expected value of  $x$  reads:

$$y = f(E(x)) + \sum_{i=1}^n \frac{\partial f}{\partial x_i} (x_i - E(x_i)) + \frac{1}{2} \sum_{i=1}^n \sum_{j=1}^n \frac{\partial^2 f}{\partial x_i \partial x_j} (x_i - E(x_i))(x_j - E(x_j)) + O(\|x - E(x)\|^3) \quad (1)$$

This Taylor expansion is used to compute the expected value and variance of the random variable  $y$ .

#### 1. First order method

The expected value of  $y$  is in this case the value given by the deterministic computation:

$$E(y) = f(E(x)) \quad (2)$$

The variance of  $y$  reads:

$$\text{var}(y) = \sum_{i=1}^n \sum_{j=1}^n \frac{\partial f}{\partial x_i} \frac{\partial f}{\partial x_j} \text{cov}(x_i, x_j) \quad (3)$$

and involves the covariance of the random variables  $x_i$  and  $x_j$ . The covariance measures the extent to which  $x_i$  and  $x_j$  vary jointly. The covariance is defined in term of the expected value of the random variables  $x_i$  and  $x_j$  as  $\text{cov}(x_i, x_j) = E(x_i x_j - E(x_i)E(x_j))$ .

## 2. Second order method

The second order method uses the curvature of  $f$  to correct the expect value of  $y$  which reads:

$$E(y) = f(E(x)) + \frac{1}{2} \sum_{i=1}^n \sum_{j=1}^n \frac{\partial^2 f}{\partial x_i \partial x_j} \text{cov}(x_i, x_j) \quad (4)$$

The same kind of corrections appear for the variance of  $y$  :

$$\text{var}(y) = \sum_{i=1}^n \sum_{j=1}^n \frac{\partial f}{\partial x_i} \frac{\partial f}{\partial x_j} \text{cov}(x_i, x_j) + \frac{1}{4} \left( \sum_{i=1}^n \sum_{j=1}^n \frac{\partial^2 f}{\partial x_i \partial x_j} \text{cov}(x_i, x_j) \right)^2 \quad (5)$$

The second order approximation is much richer. For instance, if  $x$  derives from an optimization problem and is a free optimum, the first order method does not give any information about the variance since  $\frac{\partial f}{\partial x_i} = 0$ .

## B. Computation of the derivatives

In CFD applications, the evaluation of the function of interest  $f(x)$  requires the solution of a state equation since  $f(x)$  actually reads:

$$f(x) = F(x, u(x)) \quad (6)$$

where  $x$  and  $u(x)$  are linked through the state equation

$$S(x, u(x)) = 0 \quad (7)$$

In our case, the state equation is governed by the Reynolds Averaged Navier-Stokes equations and the function of interest is typically an aerodynamic coefficient (lift coefficient, drag coefficient, pitching moment, etc. ...). The computation of the derivatives is central in the process and needs to be presented in detail.

### 1. First order derivatives

A straightforward chain rule for the first derivative of  $f$  leads to:

$$\frac{\partial f}{\partial x_i} = \frac{\partial F}{\partial x_i} + \frac{\partial F}{\partial u} \frac{\partial u}{\partial x_i} \quad (8)$$

The derivative of equation (7) with respect to  $x_i$  reads:

$$\frac{\partial S}{\partial x_i} + \frac{\partial S}{\partial u} \frac{\partial u}{\partial x_i} = 0 \quad (9)$$

We now introduce an adjoint variable  $\psi$  solution of the adjoint equation:

$$\psi^T \frac{\partial S}{\partial u} = \frac{\partial F}{\partial u} \quad (10)$$

The derivative  $\frac{\partial u}{\partial x_i}$  can be eliminated from Eq. (9) and the gradient of  $f$  is calculated as follows:

$$\frac{\partial f}{\partial x_i} = \frac{\partial F}{\partial x_i} - \psi^T \frac{\partial S}{\partial x_i} \quad (11)$$

## 2. Second order derivatives

After some calculus manipulations the Hessian of  $f$  reads:

$$\frac{\partial^2 f}{\partial x_i \partial x_j} = \frac{\partial F}{\partial u} \frac{\partial^2 u}{\partial x_i \partial x_j} + D_{ij}^2 F \quad (12)$$

In Eq. (12) the differential operator  $D_{ij}^2 \cdot$  is defined by:

$$D_{ij}^2(\cdot) = \frac{\partial^2(\cdot)}{\partial x_i \partial x_j} + \frac{\partial^2(\cdot)}{\partial u^2} \frac{\partial u}{\partial x_i} \frac{\partial u}{\partial x_j} + \frac{\partial^2(\cdot)}{\partial u \partial x_i} \frac{\partial u}{\partial x_j} + \frac{\partial^2(\cdot)}{\partial u \partial x_j} \frac{\partial u}{\partial x_i} \quad (13)$$

Inspection of Eq. (12) shows that the Hessian of  $f$  involves the second order derivatives  $\frac{\partial^2 u}{\partial x_i \partial x_j}$ . We follow

the method proposed by Giles (Ref. 2) to eliminate the second order derivatives of  $u$  in a similar manner to the elimination of the first order derivatives of  $u$  from Eq. (8). Once again the state equation plays a central role and the steps are described below.

Taking the derivative of Eq. (9) with respect to  $x_j$  leads to:

$$D_{ij}^2 S + \frac{\partial S}{\partial u} \frac{\partial^2 u}{\partial x_i \partial x_j} = 0 \quad (14)$$

Using Eq. (14), Eq. (12) can be rewritten as

$$\begin{aligned} \frac{\partial^2 f}{\partial x_i \partial x_j} &= \frac{\partial F}{\partial u} \frac{\partial^2 u}{\partial x_i \partial x_j} + D_{ij}^2 F - \psi^T \left( D_{ij}^2 S + \frac{\partial S}{\partial u} \frac{\partial^2 u}{\partial x_i \partial x_j} \right) \\ &= D_{ij}^2 F - \psi^T D_{ij}^2 S + \left( \frac{\partial F}{\partial u} - \psi^T \frac{\partial S}{\partial u} \right) \frac{\partial^2 u}{\partial x_i \partial x_j} \end{aligned} \quad (15)$$

And by definition of the adjoint  $\psi$  (Eq. (10)) we finally obtain:

$$\frac{\partial^2 f}{\partial x_i \partial x_j} = D_{ij}^2 F - \psi^T D_{ij}^2 S \quad (15)$$

### C. Practical implementation

For the practical implementation we fully rely on the Automatic Differentiation software TAPENADE<sup>7</sup> from INRIA.. Since Dassault-Aviation Reynolds Averaged Navier-Stokes code *AETHER* is used in automatic shape optimization loops the first derivatives are already available in both direct and reverse modes (see Ref. 5 for TAPENADE in reverse mode). The second order derivatives are being computed with TAPENADE.

### D. Benefits and limitations

The major benefit of the moment method arises from its moderate computational overhead. To estimate the computational effort of the moments method (after the solution of the non linear problem) we consider a case with  $n$  uncertain parameters,  $m$  outputs and a discrete state equation of size  $N$ . The main computational effort is:

- For the first order method:  $m$  adjoint equation solutions (Eq. (10) solved for each output),
- For the second order method:  $m$  adjoint equation solutions (Eq. (10) solved for each output) and  $n$  sensitivity equation solutions (Eq. (9) solved for each input).

Both the solutions of Eq. (9) and Eq. (10) involve the solution of  $N \times N$  linear systems. Efficient linear solvers are thus required. This can be challenging for large ( $N$  is typically of the order of  $10^7$  for 3D problems) sparse linear systems with multiple right hand sides on a distributed memory parallel computer. The computational effort associated to the calculation of the derivatives  $\frac{\partial F}{\partial x_i}$ ,  $\frac{\partial S}{\partial x_i}$ ,  $D_{ij}^2 F$  and  $D_{ij}^2 S$  is small compared to the solution of an

$N \times N$  linear system.

The real limitation of this approach is that it only estimates the moments which may not provide enough information to compute a probability or estimate a distribution, should the output distribution depart from a normal distribution.

## III. Monte Carlo using surrogate models

A Monte Carlo simulation would provide, in theory at least, an estimate of the probability density function of the outputs. The major drawback of Monte Carlo is the computational effort required. Each sample requires the solution of a *non linear* problem and the number of samples can be high since the convergence rate of the Monte Carlo method scales only as the reciprocal of the square root of the number of samples.

Surrogate models appear to be an elegant manner to overcome the computing time associated with Monte-Carlo simulations. The idea is extremely simple and consists of using an approximation of the expansive non linear problem for the Monte Carlo simulation. The computational advantage is evident since an evaluation of the surrogate model is performed at a negligible cost, the CPU intensive part being the construction of the model which is done once and for all.

Surrogate models can be constructed using a wide variety of techniques. In this work we investigate three different surrogate models that can be separated into local and global models.

#### 1. Local surrogate model based on a Taylor expansion

The derivatives computed for the moments method can be used to directly compute the terms of the Taylor expansion of the output functions. A *local* surrogate model is thus a *direct* byproduct of the moments method.

#### 2. Global surrogate models

The construction of a global model can be computationally expansive for a large number of parameters. Radial Basis Functions, thanks to their ability to incorporate derivatives information to improve the accuracy of the model (Ref. 6).are attractive to construct surrogate models. Kriging methods are an alternate approach for the construction of global surrogate models. By definition, Kriging methods (Ref. 7) can provide an estimate of the surrogate model error which can be used both during the construction of the model and later in its exploitation phase.

---

<sup>7</sup>URL : <http://tapenade.inria.fr:8080/>

## IV. Applications

### A. High lift configuration.

The first case considered is a very simplified analysis of the effect of the aerodynamic loads on a flap and the associated possible rotation of the flap around its hinge. We seek to evaluate the impact of the flap rotation on the lift coefficient. We consider a 2D geometry of a high lift three element airfoil and the random parameter is the rotation of the flap. Even in this simplified case the transfer function is complex. The computation of a new value of the lift coefficient for a new flap rotation requires a step of mesh deformation before the Navier-Stokes computation.

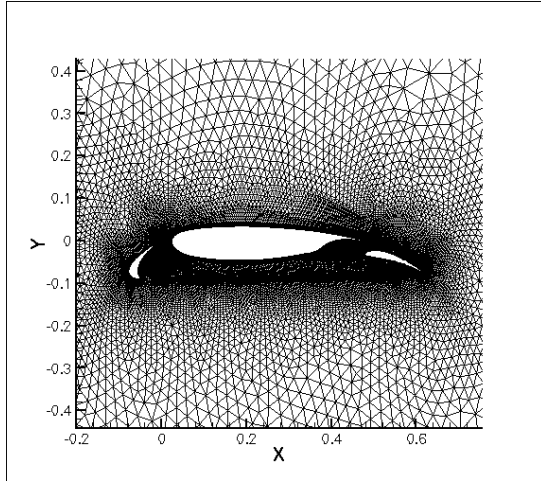


**Figure 1. Details of the Finite Element mesh around the airfoil**

case the second order derivatives are estimated using a centered finite difference formula. The variation of the lift coefficient with the flap rotation is presented in Fig. 2.

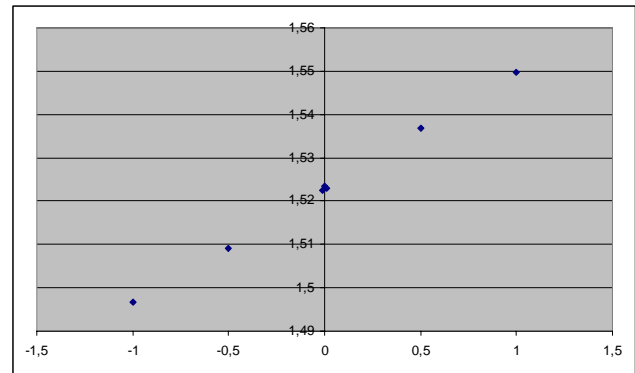
We assume a normal distribution for the flap rotation, centered around the reference position and with a standard deviation such that 95% of the samples fall between  $-1^\circ$  and  $1^\circ$ . The two propagation techniques presented above are tested and compared. The surrogate model is constructed using Radial Basis Function and 10,000 samples are used in the Monte-Carlo simulation.

Table 1 summarizes the value obtained for the mean lift coefficient and its standard deviation using a first order approximation, a second order approximation and a Monte Carlo simulation. In this case, all the methods give a similar result. This can be explained by the fact that the lift coefficient varies almost linearly with the flap angle. In this case the second derivative of the output is very small and thus the first order and second order methods are very close. Since the linear transform of a normal distribution is also a normal distribution, Monte-Carlo does not improve the predictions.

### B. Transonic airfoil.

The second application is to evaluate the impact on the drag coefficient of a geometrical deformation close to the leading edge on the suction side of an airfoil. A parametric CAD definition of the airfoil is used to generate the new geometries. In Fig. 4 we present the reference airfoil in red and the extremes of the deformation in blue and green. The airfoil considered here is a RAE2822 at Mach=0.734 and  $2.79^\circ$  angle of attack. The mesh used in this case has around 35,000 grid points. The calculations are performed with the same  $k - \varepsilon$  turbulence model as in the previous example and a step of mesh deformation is also required to evaluate a new value of the drag coefficient for each new geometry. For this case 14 different configurations have been evaluated. The effect of the geometrical deformation is presented in Fig. 5 in which the reference point is  $P_z=0.97$ ,  $C_x=0.0131$ . For this case all the surrogate models

In these computations we use a  $k - \varepsilon$  turbulence model which is integrated down to the wall. The unstructured mesh has around 60,000 grid points. A detail of the mesh around the airfoil is presented in Fig. 1. This mesh is thin enough to capture the critical details of the flow yet it allows one to perform as many simulations as necessary. The angle of attack is moderate to stay within the linear part of the lift curve. The flap rotates between  $-1^\circ$  and  $1^\circ$  around its reference configuration. Seven different flap positions have been computed ( $-1^\circ, -0.5^\circ, -0.01^\circ, 0^\circ, 0.01^\circ, 0.5^\circ, 1^\circ$ ). In this



**Figure 2. Variation of the lift coefficient as a function of the flap rotation.**

**Table 1. Comparison of mean and variance prediction for lift coefficient**

	Mean	Variance
<b>First Order</b>	1.5234	1.98e-4
<b>Second order</b>	1.5229	1.98e-4
<b>Monte Carlo</b>	1.5229	1.94e-4

presented previously have been used. The global models are constructed using only 3 points (the green dots in Fig. 5). The curve of the RBF model and the curve of the Kriging model are respectively the red dashed line and the blue dashed line in Fig. 5. The Kriging model has been constructed using the DACE Kriging Toolbox for Matlab (Ref. 8). As can be seen in Fig. 5 the RBF model and the Kriging model behave essentially in the same manner and, within their interpolation domain, their predictions are very accurate. Two examples of uncertainty propagations are performed, both assume a normal distribution around the reference point and the standard deviations of the input are respectively 0.01 and 0.02. In Fig. 5 the red box represents the region that contains 95% of the samples for the 0.02 standard deviation case. The propagation methods used here are the first order moments method, the second order moments method, Monte Carlo simulation using a first order Taylor expansion, Monte Carlo simulation using a second order expansion, Monte Carlo simulation using the RBF model and finally Monte Carlo simulation using the Kriging model. All the Monte Carlo simulations are performed using 10,000 samples. For both values of the standard deviation the same surrogate models are used.

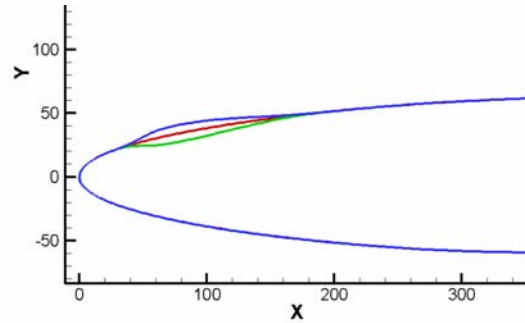


**Figure 4. geometrical deformation**

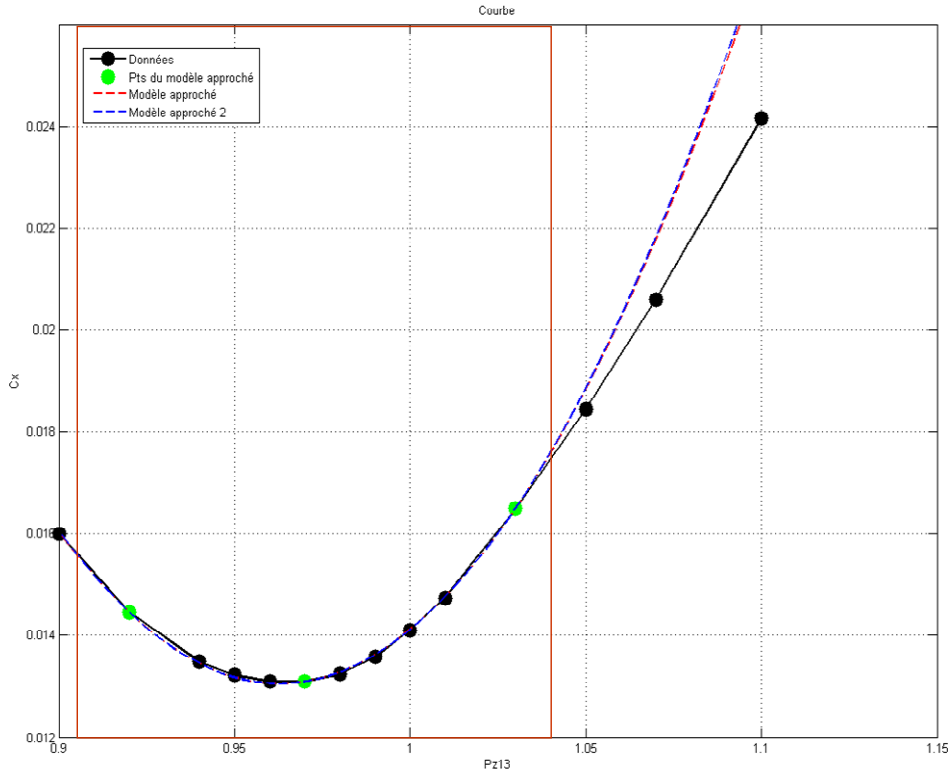


**Figure 5. Drag coefficient as a function of the geometrical deformation**

As can be seen in Fig. 5 the drag coefficient is a non linear function of the geometrical deformation. This example is thus more discriminating for the propagation methods than the previous one. The results for the two propagation cases are summarized respectively in Table 2 ( $\sigma_{input} = 0.01$ ) and Table 3 ( $\sigma_{input} = 0.02$ ). In both cases the results clearly show two types of behavior. On the one hand the linear method: first order method and Monte Carlo using a first order Taylor expansion and the non linear method on the other hand. The two linear methods give, as expected, the same results in both cases. It is worth noting that in this example, the deterministic

value of the drag coefficient does not correspond to the expected value of the drag coefficient considered as a random variable; there is a difference greater than 3 drag counts between the linear methods and the non linear methods for the case  $\sigma_{input} = 0.02$ .

**Table 2 Comparison of mean and variance prediction for drag coefficient ( $\sigma_{input}=0.01$ )**

	Mean	Std deviation
<b>First order</b>	130.94e-4	0.77e-4
<b>Second order</b>	131.71e-4	1.33e-4
<b>MC Taylor 1</b>	130.94e-4	0.77e-4
<b>MC Taylor 2</b>	131.69e-4	1.29e-4
<b>MC RBF</b>	131.70e-4	1.54e-4
<b>MC Kriging</b>	131.70e-4	1.56e-4

**Table 3 Comparison of mean and variance prediction for drag coefficient ( $\sigma_{input}=0.02$ )**

	Mean	Std deviation
<b>First order</b>	130.94e-4	1.55e-4
<b>Second order</b>	134.00e-4	4.60e-4
<b>MC Taylor 1</b>	130.95e-4	1.55e-4
<b>MC Taylor 2</b>	134.02e-4	4.52e-4
<b>MC RBF</b>	133.97e-4	4.81e-4
<b>MC Kriging</b>	134.04e-4	4.95e-4

The non linear methods give the same results for the mean value in both cases. The predictions of the standard deviation are more scattered. We have basically two families of behavior: second order moments method and Monte Carlo using a second order Taylor expansion for one and the Monte Carlo with an RBF model or a Kriging model for the other. Further investigations are needed to understand these differences.

## V. Conclusion and perspectives

In this paper we present some preliminary results on uncertainties propagation through a CFD simulation. The transonic example clearly shows the advantage of considering a second order method and justifies the extra work that is involved for the computation of the second order derivatives. It is, once again, important to stress that the information about the first two moments does not suffice to determine a confidence interval if the output distribution departs too much from a normal distribution, whilst the empirical distribution obtained with Monte-Carlo will allow one to estimate the confidence interval. In the latter case it will then be necessary to assess the statistical error between the actual model (Navier-Stokes) and the surrogate model. It is also important to keep in mind that the difficulty and the computing cost of building a surrogate model grows exponentially with the number of parameters. The moments method only requires *one solution of the non linear system* and additional solutions of linear systems. This feature is very appealing for industrial applications. Given the complementarities of the two approaches both are required in our toolbox.

## Acknowledgments

Part of this work was supported by the project NODESIM-CFD "Non-Deterministic Simulation for CFD-based Design Methodologies" funded by the European Community represented by the CEC, Research Directorate-General, in the 6th Framework Programme, under Contract No. AST5-CT-2006-030959.

## References

- <sup>1</sup> *Guide for the verification and validation of computational fluid dynamics simulation*, AIAA Guide, G-077-1998, 1998.
- <sup>2</sup> Ghate, D.P., and Giles, M.B. "Efficient Hessian Calculation using Automatic Differentiation," *25<sup>th</sup> AIAA Applied Aerodynamics Conference*, June 25-28 2007, Miami, USA.
- <sup>3</sup> Martinelli, M., "Sensitivity Evaluation in Aerodynamic Optimal Design," Ph.D. Dissertation, Scuole Normale Superiore di Pisa, 2007.
- <sup>4</sup> Martinelli, M., Dervieux, A., and Hascoët, L., "Strategies for computing second order derivatives in CFD design problems," *Proceedings of the West East high Speed Flow Conference*, Nov. 19-22 2007, Moscow, Russia.
- <sup>5</sup> Hascoët, L., and Araya-Polo, M., "The adjoint data Flow Analysis: Formulation, Properties and Applications" *Automatic Differentiation, Application, Theory and Tools H.M. Bücker, G. Corliss, P. Horland, U. Naumann, B. Norris (Eds) Lecture Notes in Computational Sciences and Engineering*, Springer 2005.
- <sup>6</sup> Kybic, J., Blu, Th., and Unser, M., "Generalized Sampling: A variational Approach. Part II - Applications," *IEEE Transactions on Signal Processing*, vol 50, n° 8, August 2002, pp1977-1985.
- <sup>7</sup> Giunta, A., "Aircraft multidisciplinary design optimization using design of experiments theory and response surface modelling methods," Ph.D. Dissertation, Virginia Polytechnic Institute and State University, May 1997.
- <sup>8</sup> Lophaven, S.N., Nielsen, H.B., and Sondergaard, J., "DACE a Matlab Kriging Toolbox," *Technical Report*, IMM-TR-2002-12, Technical University of Denmark, 2002.